PHYSICAL REVIEW D

PARTICLES AND FIELDS

THIRD SERIES, VOLUME 42, NUMBER 4 15 AUGUST 1990

Search for an intermediate-range composition-dependent force coupling to $N-Z$

P. G. Nelson,* D. M. Graham, and R. D. Newman

Department of Physics, University of California, Irvine, California 92717

(Received 26 February 1990)

We report a search for composition dependence in the forces acting on two test masses made primarily of lead and copper, due to an attracting mass made primarily of lead. The test masses are mounted on a torsion balance of high symmetry. The attracting mass is a 320-kg lead ring in an aluminum shell, positioned so that the torsion balance lies on the ring's axis at a distance from its center approximately equal to $\sqrt{3/2}$ times the ring's mean radius. When the ring is moved periodically between symmetric positions on opposite sides of the balance, the resulting change in gravitational field experienced by the balance is spatially uniform to a very high degree: all derivatives of the change in field at the center of the balance vanish through third order. We find the apparent gravitational force per unit mass on the two test masses due to the attracting ring mass to be equal to within 1.1 ± 1.2 ppm. Assuming a parametrization of a composition-dependent force in the notation of Fischbach, we find $\xi=(5.7\pm6.3)\times10^{-5}$ for $\theta_5=90°$ ($N-Z$ coupling), $\xi=(-1.2\pm1.3)\times10^{-3}$ for $\theta_5=0°$ (B coupling).

I. INTRODUCTION

The possible existence of a composition-dependent force weaker than gravity, of macroscopic but finite range, has been extensively explored in the past five years. Evidence that such a force was manifested in the classic equivalence principle test of Eötvös[1] was found in a reanalysis of that experiment by Fischbach and his collaborators.[2,3] Two experiments[4,5] have since given further evidence for an anomalous composition-dependent force, while other experiments[6–18] find no anomaly and strongly constrain the values of strengths and couplings of a possible anomalous composition-dependent force.[19]

A composition-dependent force, associated with the exchange of a single boson of very low mass, might couple to the total baryon content B of the interacting masses or to the difference $N-Z$ in their total proton and neutron content (or equivalently for neutral atoms, to $B-2L$). The $N-Z$ dependence could reflect a coupling to isospin (I_3), although this possibility has been strongly constrained by Nieto[20] based on the nonobservation of K-meson decay into the supposed mediating boson. A parametrization of an anomalous composition-dependent force superimposed on gravity may be given in the notation of Fischbach *et al.*:[2]

$$V=\frac{-Gm_1m_2}{r}(1-\xi q_1q_2e^{-r/\lambda}) , \tag{1}$$

where

$$q=\frac{1}{\mu}[B\cos\theta_5+(N-Z)\sin\theta_5] . \tag{2}$$

Here ξ and λ represent the strength and range of an anomalous interaction, while q_1 and q_2 are the anomalous charges of the interacting masses m_1 and m_2, μ is the mass of the interacting object expressed in units of the hydrogen-atom mass, and θ_5 is a mixing angle specifying the relative strengths of coupling to B and $N-Z$.

Our experiment uses a controlled source mass of known composition and geometry to search for a composition-dependent force acting on test masses mounted on a torsion balance. The experiment was designed to be particularly sensitive to a force coupling to $N-Z$. To this end, the attracting mass was made primarily of a material with large neutron excess (lead), and the two test masses are copper and (primarily) lead—materials with a relatively large difference in fractional neutron excess, and similar densities.

II. EXPERIMENTAL TECHNIQUE

A. Principle of the experiment

The basic principle of our experiment is illustrated in Fig. 1. An attracting mass in the form of a ring is moved periodically from one side of a torsion balance to the other. A composition-dependent force on two test masses mounted on the balance would produce a torque on the balance which reverses sign when the attracting mass is

 ©1990 The American Physical Society

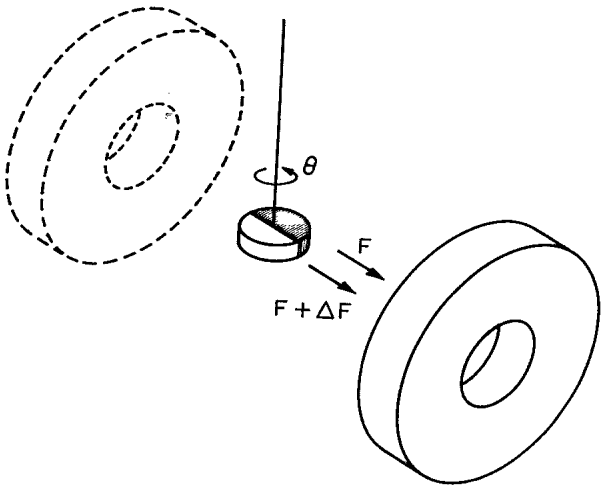

FIG. 1. Method of the experiment. The torque change on the balance made of two different materials is monitored as the ring-shaped source mass is moved periodically between the indicated positions. Figure is not to scale.

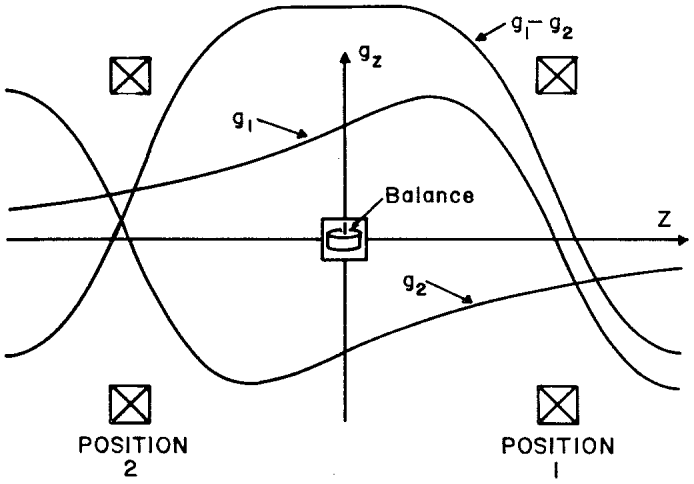

FIG. 2. Principle of the highly uniform gravitational difference field. A ring mass at position 1, producing the axial field g_1 whose second derivative vanishes at the center of the torsion balance, is moved to position 2 where its axial field becomes g_2. All derivatives of the difference field $\mathbf{g}_1-\mathbf{g}_2$ vanish through third order at the origin, leading to a highly uniform field difference at the position of the balance.

moved. The resulting change in equilibrium angle θ of the balance is sensed by an optical lever (autocollimator) viewing a mirrored surface of the balance.

B. Control of gravitational gradients

A major difficulty in an experiment of this kind can arise from the coupling of spatial derivatives of the Newtonian gravitational field of the attracting mass to mass multipole moments of the balance, producing torque changes on the balance which simulate an anomalous force. A key feature of our experiment is the use of a ring attracting mass in a way which greatly reduces this danger. We exploit the fact that there exists a position on the axis of a ring such that the *change* in gravitational field produced by moving the ring to a symmetric location on the far side of this position is spatially uniform to a remarkable degree: assuming a homogeneous and geometrically perfect mass ring, all spatial derivatives of the change in field vanish through third order. For a general ring of finite thickness this position is the point at which the second derivative of the axial gravitational field vanishes (first and third derivatives of the change in field associated with moving the ring then vanish by symmetry arguments). For a thin ring of radius R this position is at a distance $z=\sqrt{3/2}R$ from the center of the ring. Since it is only the change in field to which the torsion balance responds, this experimental method is effectively equivalent to using an attracting mass whose gravitational field is extremely uniform. Figure 2 illustrates the cancellation in axial field derivatives for the difference field of a ring.

The Newtonian interaction of a ring attracting mass with the gravitational multipole moments of a torsion balance is conveniently discussed with a multipole formalism which closely parallels that commonly applied to electrostatic interactions of charge distributions.[21] The change in gravitational potential in the region of the balance due to the attracting mass ring may be written as

$$\Delta\Phi=\sum_{l=0}^{\infty}\sum_{m=-l}^{l}\Delta a_{lm}r^{l}Y_{lm}(\theta,\phi)\ , \tag{3}$$

where the coefficients a_{lm} are given in terms of the attracting mass distribution ρ_s by

$$a_{lm}=\frac{-4\pi G}{2l+1}\int\frac{\rho_s(\mathbf{r})}{r^{l+1}}Y^{*}_{lm}(\theta,\phi)d^3r \tag{4}$$

and Δa_{lm} is the change in a_{lm} when the ring is moved from one side of the balance to the other. We may demonstrate as follows that Δa_{lm} vanishes for $l=2$, 3, and 4, for any choice of polar axis. Consider Eq. (3), choosing the polar axis to be the symmetry axis of the ring. The azimuthal symmetry of the ring's field implies that Δa_{lm} vanishes for $m\neq 0$. The vanishing of the first three derivatives of the axial difference field Δg_z implies that $\partial_r^{(n)}\partial_r\Delta\Phi(\theta=0)=0$ for $n=1$, 2, and 3, which in turn implies that Δa_{l0} vanishes for $l=2$, 3, and 4. Since for this polar axis Δa_{lm} vanishes for all m if $l=2,3,4$ it follows that this is true for any polar axis, and in particular for a vertical polar axis (since a rotation only mixes those coefficients having the same l values in the expansion). It then follows that all spatial derivatives of the gravitational field difference $\nabla(\Delta\Phi)$ vanish through third order, in any coordinate system (including a Cartesian system).

Taking the polar axis to be vertical and defining the mass multipole moments of the balance in a body-fixed coordinate system (r',θ',ϕ') by

$$q_{lm}=\int\rho(\mathbf{r}')r'^{l}Y^{*}_{lm}(\theta',\phi')d^3r' \tag{5}$$

the potential energy of the balance in the field of the ring

is given by

$$U(\Psi)=\sum_{l=0}^{\infty}\sum_{m=-l}^{l} a_{lm}^{*}q_{lm}e^{im\Psi}\ , \tag{6}$$

where Ψ is the azimuthal position of the ring in the body-fixed coordinate system of the balance. Differentiating this expression with respect to Ψ then gives the torque on the balance:

$$\tau(\Psi)=\sum_{l=0}^{\infty}\sum_{m=-l}^{l} ima_{lm}^{*}q_{lm}e^{im\Psi}\ . \tag{7}$$

We note in passing that a further differentiation of Eq. (7) with respect to Ψ gives the effective change δk in torsion constant of the balance associated with the gravitational field of the attracting mass:

$$\delta k(\Psi)=\sum_{l=0}^{\infty}\sum_{m=-l}^{l} -m^{2}a_{lm}^{*}q_{lm}e^{im\Psi}\ . \tag{8}$$

This expression is of use in experiments which explore gravitational interactions by measuring changes in the oscillation frequency of a torsion balance as a function of the orientation of an attracting mass.

From Eq. (7) we see that the change in torque $\Delta\tau(\Psi)$ when the ring is transported (Ψ increased by 180°) is given by

$$\Delta\tau(\Psi)=\sum_{l=0}^{\infty}\sum_{m=-l}^{l} im\,\Delta a_{lm}^{*}q_{lm}e^{im\Psi}\ , \tag{9}$$

where Ψ is the initial azimuthal position of the ring relative to the balance and Δa_{lm} is the difference in the a_{lm} calculated for the two ring positions.

For a perfectly machined and positioned ring we have shown that $\Delta a_{lm}=0$ for $l=2,3,4$ while for a rotationally symmetric balance $q_{lm}=0$ for all nonzero m. Thus either of these conditions would cause the Newtonian torque change $\Delta\tau$ to vanish to a very high order, while the actual value of $\Delta\tau$ will be proportional to the product of small realistic finite values of Δa_{lm}^{*} and q_{lm}. The result is a very fault-tolerant system: with reasonable care in the production of both balance and ring, the result of first-order imperfections in each component is a very small second-order error due to Newtonian field derivative couplings to the balance.

C. Experimental apparatus

A scale drawing of the full apparatus is presented in Fig. 3. The apparatus operates in an unventilated subbasement chamber which is sealed by a styrofoam roof plug for thermal stability. The mass ring is suspended from a horizontal turntable above the balance. This turntable is linked by a belt drive and vertical shaft to a computer-controlled stepper motor above the thermal insulating plug which serves to rotate the turntable, transporting the attracting mass.

The lead component of the attracting mass is a 321-kg ring of 60.8 cm outside diameter (O.D.), 29.5 cm inside diameter (I.D.), and 12.5 cm thickness, assembled from five thin rings of the same O.D. and I.D. each machined to 2.5 cm thickness from plates rolled to this approximate thickness from 10-cm-thick cast sheets. The rolling process was invoked to improve the homogeneity of the lead. Extensive ultrasound scans were made of each of the five component rings before assembly, both radially and in the axial dimension, to test its homogeneity; the sound velocity was found to not deviate from the mean for each type of scan by more than a part per thousand over all five plates. Since the sound velocity should scale roughly as the square root of material density, we interpret these results as putting a limit of about two parts per thousand on density inhomogeneity averaged over the path of each scan. In addition, gamma transmission scans were made of all five plates, with results which were less precise than but consistent with results of the ultrasound scan. The lead subrings mount on an aluminum hub ring, and are flanked by 2-cm-thick aluminum side plates. A set of eight brass rods links the side plates together near their

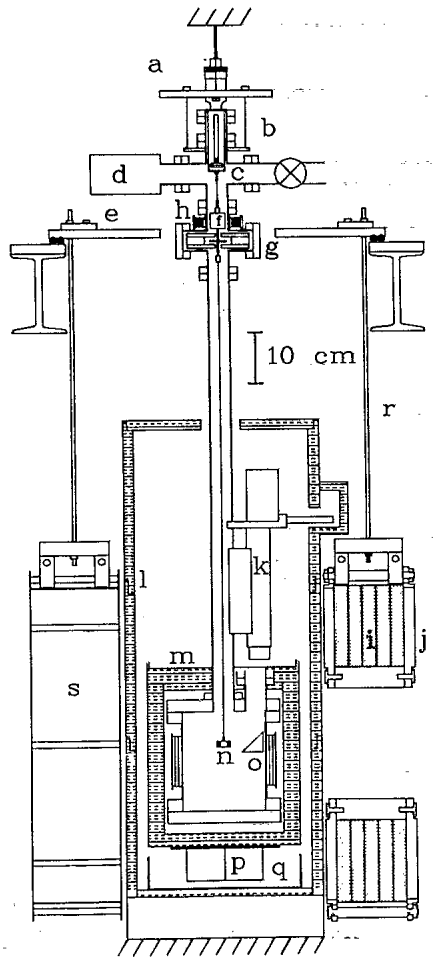

FIG. 3. Scale drawing of the apparatus: (a) balance housing suspension wires, (b) θ zero adjustment, (c) stiff upper fiber, (d) ion vacuum pump, (e) ring transport turntable, (f) damping assembly, (g) pendulum mode damping magnets, (h) magnetic induction torsional mode damping, (i) lead attracting mass ring, cross section, (j) aluminum ring case, (k) optical lever θ readout, (l) stationary magnetic and thermal shielding, (m) magnetic and thermal shielding, suspended with housing, (n) balance with test masses, (o) mirror, (p) damping fins for balance housing, (q) oil-filled pan, (r) ring suspension rod, and (s) dummy ring.

outer diameter and serve as hangers for suspending the ring. The total 367-kg mass of the assembled ring is 87% lead, 12% aluminum, and 1% brass. Dimensional uniformity of the lead ring was maintained to 15 μm; the whole assembly deviated nowhere by more than 50 μm from its intended form.

An analytical expression for the axial field due to each of the ring's components was computed and summed to give the total ring field as a function of axial position. The second derivative of this function was then computed, and the axial position at which this second derivative vanishes determined. This point, at which the balance should be located to achieve the flat difference field when the ring is transported, is at a distance calculated to be 26.822 cm from the geometric center of the finite thickness ring. A "dummy" ring was suspended opposite the real ring, from an identical hanger. This ring had the same dimensions and aluminum surface composition as the real ring, but only 1% of its mass. Its purpose was to minimize possible influences of ring position on convection air currents in the instrument pit.

The arrangement of the test masses in the torsion balance is indicated in Fig. 4. The lead mass is sandwiched between two identical aluminum pieces so that the combined height and mass of the aluminum-lead system is the same as that for the copper test mass. The masses of the copper, lead, and aluminum components are, respectively, 12.97, 11.84, and 1.13 g. Each piece has a semicircular inside radius of 0.384 cm and outside radius 1.078 cm. The total height of the test masses is 0.914 cm. The dipole moment of the copper test mass alone is 6.49 g cm, corresponding to $q_{11}=2.25$ g cm. The masses rest in a copper tray of hexagonal symmetry. The total mass of the balance is 49.3 g; its moment of inertia is 43.1 g cm^2. A set of short 66-mg copper threaded slugs are located in six tapped holes around the periphery of the balance; screwing these slugs up or down allows compensation for a measured q_{21} mass multipole moment. In the present experiment we found the initially measured value of q_{21} to be small enough that no compensation was necessary.

There are three levels of suspension of the balance.

(1) The whole vacuum housing containing the balance, along with the vacuum pump and optical system, is suspended by wires so that the balance's position relative to its housing is minimally affected by floor tilt associated with the transport of the ring mass.

(2) Within the vacuum housing a 3.6-cm-long, 380-μm-diameter phosphor bronze wire suspends a "damping assembly" from which the main torsion fiber is suspended (Fig. 5). On this intermediate assembly two modes of damping are applied: (a) Pendulum motion of the balance below is transmitted to the assembly causing a horizontal copper disk to move between the pole pieces of two fixed "C" magnets, providing passive damping of the pendulum modes, and (b) the torsional mode of the balance is critically damped by an active feedback system, using magnetic induction to generate controlled rotations of a vertically oriented copper tube secured to the damping assembly. To accomplish this, a pair of air-core coils external to the vacuum system, flanking the copper tube, is driven with an ac current, while another pair of coils

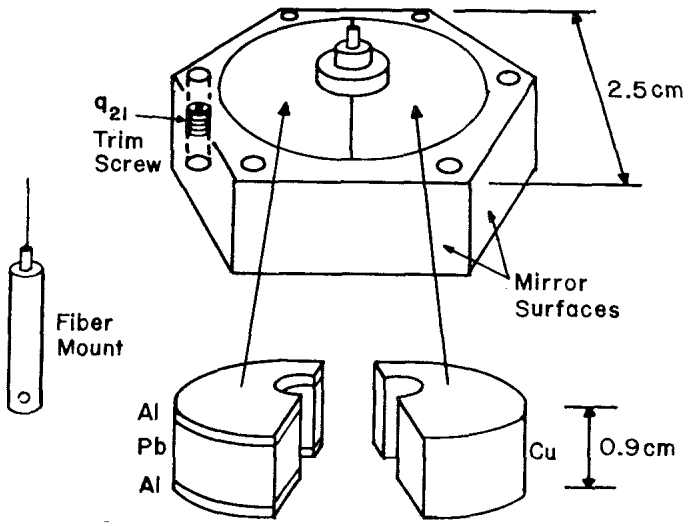

FIG. 4. Arrangement of the test masses in the torsion balance.

on an orthogonal axis is driven with an ac current 90° out of phase with the first, with a magnitude and phase sign determined by the balance angular velocity signal derived from the optical lever. The resulting magnetic field rotates in a horizontal plane in the region of the copper tube on the damping assembly, producing a torque which

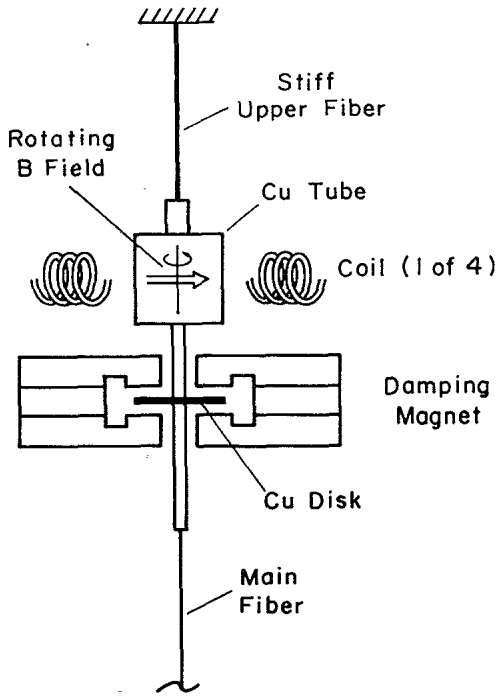

FIG. 5. The damping assembly at the top of the torsion fiber. Eddy currents in the copper disk damp pendulum motion of the balance. A rotating magnetic field produced by ac currents in two orthogonal coil pairs (one pair shown) exerts a torque on the copper tube thus controlling the angular position of the fiber support to critically damp torsional oscillations of the balance.

controls its angular position, thus applying a controlled effective torque to the balance at the lower end of the main fiber. Critical damping of the torsional mode was readily achieved. Applying the torsional damping torque in this fashion avoids the large tilt sensitivity often associated with damping methods which apply electrostatic torques directly to the balance.

(3) Finally, the balance itself is suspended from the damping assembly by a 93-cm-long, 25-μm-diameter tungsten wire of torsion constant 0.070 dyn cm/rad, in a vacuum maintained by an 8 l/s ion pump at $<8\times10^{-7}$ Torr measured at the pump. The undamped Q of the torsional oscillation is about 3200. The torsional period is 157 sec.

The angular position of the balance is sensed by an optical lever which images an infrared light-emitting-diode (LED) source onto a split photodiode after reflection from one of the polished faces of the balance. The light source and detector are mounted in the focal plane of the lens on a plate which may be translated by remotely controlled micrometers to align and calibrate the system.

The suspended vacuum chamber carries with it two spaced layers of magnetic shielding, annealed after fabrication. Two additional layers of spaced magnetic shielding surround the balance housing, supported from the floor. Between the layers of magnetic shielding is foam thermal insulation and layers of copper shielding to help minimize the effects of temperature gradients in the pit.

III. DATA

A. Data collection

The experiment was automated by a PC computer which recorded the optical lever signal as well as data from seven thermistors, a two-axis tiltmeter, and a two-axis fluxgate magnetometer, and also controlled the transport of the mass ring.

A data collection run begins with the mass ring in an angular position ψ relative to the balance (Fig. 6). The balance angle signal is recorded at 10-sec intervals for a period of 7 min; then the ring is transported to the position $\psi+180°$. The transport takes about 5 min, and after

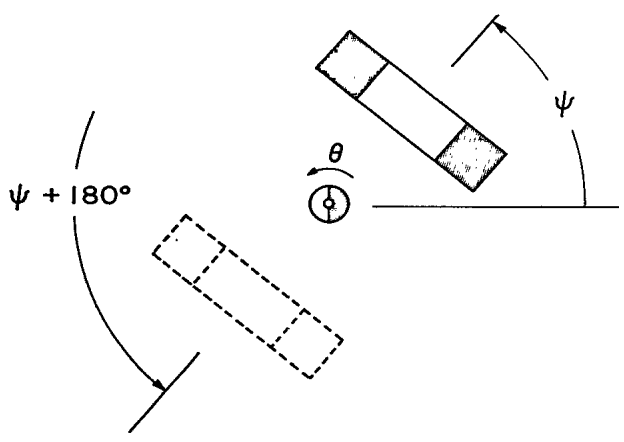

FIG. 6. Definition of ring orientation ψ and balance equilibrium angle θ.

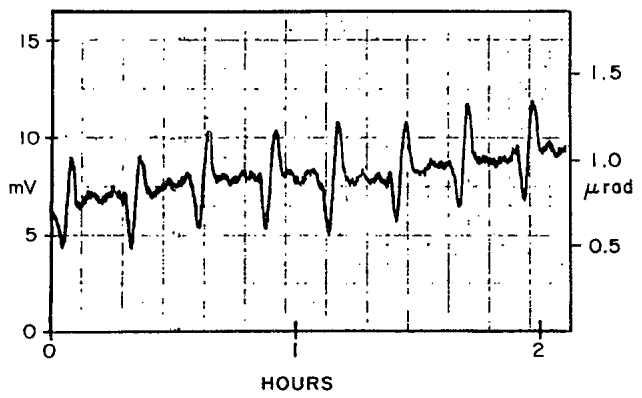

FIG. 7. Sample of the torsion balance θ signal displayed by a chart recorder. The bipolar peaks, occurring twice per ring roundtrip cycle, are due to the coupling of the a_{22} ring field moments to the small (nominally zero) balance q_{22} moments as the ring is transported.

an additional 3-min delay (settle-in period) data are sampled for 7 min at the new position. The ring is then transported in the same direction until it reaches its original position. A set of typically 20 such cycles constitutes a "run." A sample chart recorder record of this data is shown in Fig. 7. The signal-averaged data from a typical run are displayed in Fig. 8. The signal has a linear drift with time of about 250 nrad/h. The bipolar signal seen in Figs. 7 and 8, occurring twice per ring roundtrip cycle, is the response of the balance to coupling of its small (nominally zero) q_{22} moment to the a_{22} moment of the ring field as the ring is transported; while the difference Δa_{22} in a_{22} for the ring at the beginning and end of each transport is designed to be zero, the ring has a finite a_{22} at any given position.

The signal of interest is the net change $\Delta\theta(\psi)$ in balance equilibrium angular position θ when the ring is transported:

$$\Delta\theta(\psi)=\theta(\psi)-\theta(\psi+180°)\ , \tag{10}$$

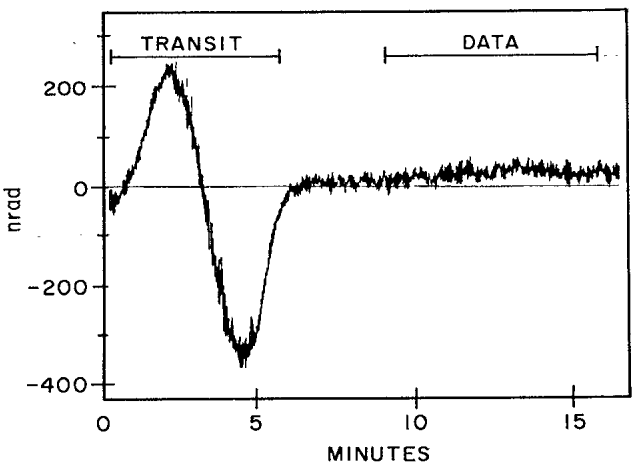

FIG. 8. The balance θ signal for one half of a roundtrip cycle, averaged over 14 roundtrip cycles. The periods of ring transport and data sampling are indicated above.

The average value and statistical uncertainty of this quantity for each run were obtained by first subtracting a cubic background for $\theta(t)$ (the balance equilibrium position as a function of time), and then computing the mean and variance of the quantities: $\Delta\theta_i=\theta_i-(\theta_{i+1}-\theta_{i-1})/2$ for average values of θ in successive half cycles, correcting the variance for redundancy in shared data between the $\Delta\theta_i$. (Results obtained without the background subtraction were not significantly different.)

Several runs were taken and averaged for each of four angles ψ to form data set I. A second data set (II) was taken after interchanging the positions of the real and dummy mass rings on the two hangers of the transport mechanism and also rotating the real ring by 180° around its symmetry axis. Taking an unweighted average of data from the two sets for each angle ψ then accomplishes three things: (1) Possible signal contributions from the transport mechanism, gravitational or otherwise, will have opposite phase for the two data sets and thus cancel for the average of sets I and II; (2) the contribution of ring mass inhomogeneity to the Δa_{21} in Eq. (9) is partially canceled; and (3) a possible net signal associated with the bipolar q_{22} excitation during transport, arising because the transport differs slightly from 180° for one choice of ring hanger, will be canceled when averaged with data obtained using the other hanger position, for which the transport difference from 180° will have the opposite sign.

Data were taken for 27 runs of about 10 h each, distributed roughly equally among $\psi=45°$, 90°, 135°, 180°, and ring configurations I and II. One run was rejected because it was necessary to enter the pit, and six other runs were truncated to remove a single block of noisy data (usually at the end of an overnight run when nearby construction activity dramatically increased the noise level). The total run time was 260 h, with a total of 926 ring transports.

B. "Blind" data analysis

To minimize the risk of subtle experimenter bias in the selection of data and analysis technique or in error estimation, we conducted the data analysis in such a way that we could not know whether we were seeing a "fifth force" signal until we had finalized the data analysis and completed the error budget. (We made some deviations from this principle in computing the final error budget, as discussed later.) The expected signal for a "fifth force" is a balance response to ring transport of the form

$$\Delta\theta(\psi)=A_5\sin\psi\ . \tag{11}$$

To disguise a possible real signal of this sort, whenever our computer determined a value of $\Delta\theta(\psi)$ it added to it the quantity $X\sin\psi$ where the value of X was not known to the experimenters. The computer reported the value of $F(\psi)=\Delta\theta(\psi)+X\sin\psi$ which was then averaged over data sets as if it were an unaltered signal. All checks which might have been made of the unaltered data could equally well be made of the altered data, such as checks of its reproducibility and of its sensitivity to deliberately produced magnetic fields, temperature gradients, or tilts, as well as tests of the requirement that $F(45°)=F(135°)=F(90°)/\sqrt{2}$ and that $F(0°)=0$ within assigned uncertainties. We then fit the averaged $F(\psi)$ to the function $A'\sin\psi$, with the result $A'=A_5+X=(-32.0\pm2.1)$ nrad, where A' is the unresolved sum of the "fifth force" signal A_5 and the as yet unrevealed term X, and the uncertainty is statistical only. The values for A' determined from data sets I and II separately, corresponding to different ring azimuthal orientations and reversed positions relative to the transport mechanism, are, respectively, -32.0 ± 3.4 and -31.5 ± 2.3 nrad; comparison of these values shows no evidence for a signal contribution due to the ring transport mechanism or to mass inhomogeneity of the ring. The slight difference between the average of these two values for A' and the value quoted reflects the fact that the latter value comes from a fit in which values of F for each ψ are taken to be an unweighted average of the values for that ψ from data sets I and II.

An additional 200 h of data (23 data runs) were collected to check for the presence of sources of systematic error; the results of these runs are discussed below.

IV. SYSTEMATIC UNCERTAINTIES

A. Magnetic coupling

Limits on a signal due to interaction of magnetic moments in the mass ring with magnetic properties of the balance were obtained as follows.

(1) The horizontal component of the magnetic moment of the balance was determined to be 5×10^{-6} erg/G, by measuring the response of the unshielded balance to an electromagnet in two different orientations relative to the balance.

(2) The horizontal components of the magnetic field associated with the mass ring at a position corresponding to that of the balance were estimated with a two-axis fluxgate magnetometer placed on the axis of the ring on the side opposite the balance. It was found that the magnetic field change associated with the mass ring was less than 3×10^{-5} G.

(3) The effectiveness of the four-layer magnetic shielding in attenuating very small field changes was investigated using the fluxgate magnetometer inside the shielding and a small cycled electromagnet in various orientations outside the shield. It was found that a field change 16 times larger than that associated with the ring was attenuated to less than 4×10^{-7} G. Taking this conservative limit on ring-associated magnetic field change experienced by the balance, along with the measured horizontal magnetic moment of the balance, a limit of 0.06 nrad was obtained for magnetic contributions to an observed signal associated with any permanent magnetic moment of the balance.

Any magnetic moment induced in the balance by the ring-associated field would be far less than that which would have been induced by the electromagnet used in measuring the effective magnetic moment of the balance, and hence may be neglected. A vertical, off-axis magnetic dipole in the balance (permanent or induced) could in-

duce a torque on the balance via couplings to horizontal gradients in the vertical component of magnetic fields associated with the attracting mass. No test was made for such a coupling. However, a gradient-associated torque of this kind due to a vertical dipole would be expected to be smaller than direct torques on a horizontal dipole having comparable magnitude, by a factor on the order of the ratio of balance dimension to attracting mass distance, and hence an order of magnitude smaller than the already completely negligible possible effect of the measured horizontal dipole moment of the balance.

B. Tilt effects

The floor tilt associated with ring transport during normal data taking was monitored by tiltmeters and found to be 600 nrad. The tilt attenuation due to the balance housing suspension was measured to be a factor of at least 500, and the tilt sensitivity of the balance itself was measured to be 0.1 μrad of apparent torsion balance rotation per microradian of balance housing tilt. Combining these numbers implies a negligible signal contribution from tilt of 0.14 nrad.

C. Thermal effects

Thermistors mounted outside of the thermal shielding surrounding the balance, positioned so that they were less than 0.5 cm away from the mass ring for one of its orientations, indicated a temperature when the true ring was present which differed by an average of 0.02 K from its value when the ring was interchanged with the dummy ring. This asymmetry suggested a potential source of systematic error. To explore this we made data runs after heating the ring for several hours to the point that the temperature difference recorded by the thermistors increased to 2.4 K. This produced a significant apparent signal of 71 ± 13 nrad, which if scaled linearly to the 0.02-K mean temperature differential normally observed would imply a one sigma limit to an error signal of 0.7 nrad. The decrease in apparent signal magnitude with time during this test, as the ring cooled, was consistent with a linear dependence of signal on ring temperature, but could not definitely establish such a dependence. Since linear scaling may be a dangerous assumption, and because of the unavoidable uncertainty in modeling for the source of the thermal systematic, we multiplied the 0.7-nrad error estimate by a safety factor of about 3 and assigned an uncertainty of 2.2 nrad to thermal sources of error.

D. Suspension asymmetry and electronic asymmetry effects

If the intermediate damping assembly in the double balance suspension deviates from azimuthal symmetry so that the lower torsion fiber is not coaxial with the upper support fiber, the Newtonian gravitational force of the attracting mass acting on the balance can produce a torque twisting the upper fiber through an angle which is transmitted to the balance, simulating an anomalous signal. To minimize such effects the top suspension fiber was made torsionally very stiff (2.2×10^4 dyn cm/rad) and care was taken to keep the upper and lower fibers as close to coaxial as possible (the lateral shift between the axes was 0.007 cm). The residual effect of this error mechanism was estimated to be a negligible signal contribution of 0.25 nrad.

A set of runs was made with the optical lever light source turned off, to test for possible electrical coupling between the ring transport system and the signal channel electronics that might simulate a true signal. A preliminary test suggested a significant effect equivalent to (-6.5 ± 2.2) nrad. However, a subsequent much more thorough set of "light-off" runs, including two runs at each of the four initial ring orientations, repeated for both ring positions relative to the transport mechanisms (data set types I and II), gave no evidence for a significant effect in any subset of the runs, and yielded a limit of 1.5 nrad for this type of error.

E. Newtonian gravitational couplings: experimental tests

Numerous experiments were performed to test the symmetries of our mass configurations and to test our analysis procedures. The type and purpose of these experiments are summarized in Table I. In some runs, the ring was replaced with a 40-kg lead cube suspended at various heights above the median plane of the balance. In some runs, the balance was deliberately made asymmetric by the addition of three 1.27-cm-long, 1.54-g copper posts with short threaded extensions which screwed into the tapped balance holes indicated in Fig. 4, at 120° intervals. Two of the posts were screwed into the balance from the top and extended upward; the third extended downward from below. We refer to this configuration as the "augmented balance" in the following text.

We discuss in turn the four types of experiments indicated in Table I.

(1) Ring attracting mass with unmodified balance. Runs under these conditions constituted the anomalous force search discussed in previous sections of this paper.

TABLE I. The type and purpose of experiments performed with the torsion balance to test mass symmetries, analysis procedures, and instrument calibration.

	Ring source mass	Cube source mass
Unmodified balance	Search for anomalous force	Test of balance symmetry (measures q_{lm})
Augmented balance	Test of ring symmetry (measures a_{lm})	Test of analysis procedure; calibration

(2) Cube attracting mass with unmodified balance. This served to test the symmetry of the balance in the form in which it was used in the anomalous force search. The multipole moments q_{lm} of the balance for $l=2$ and 3 were experimentally determined by replacing the mass ring with a 40-kg lead cube which was rotated in 30° steps for six full revolutions around the balance by the same transport mechanism which normally moved the ring. The mean balance angular equilibrium position was determined for each of the 12 azimuthal cube positions around the balance. This was done in three runs, for three different heights of the lead cube relative to the balance ($z=-1.3$, 9.4, and 20.1 cm). The angular balance displacements were converted to equivalent torques and fit to equations of the form

$$\tau(\Psi)=\sum_{l=0}^{\infty}\sum_{m=-l}^{l} ima^{*}_{lm}q_{lm}e^{im\Psi}\ , \tag{12}$$

where Ψ is the azimuthal angle of the lead cube relative to the balance and the quantities a^{*}_{lm} characterizing the source mass distribution are computed using Eq. (4) separately for each of the three cube heights. In principle our data set allows the determination of q_{lm} for $l=2$, 3, and 4, $m=1$, 2, and 3. In practice, the sensitivity to the very small couplings for $l=4$ was too small to give reliable results and we constrained the fits to include only $l=2$ and 3. The magnitudes of the resulting q_{lm} are indicated in Table II. The measured magnitude of q_{31} is in satisfactory agreement with the calculated value of 0.20 associated with the symmetry in vertical mass distribution between the copper test mass and the lead-aluminum sandwich, but differs in phase by 56°±11° from the expected value. We attribute this discrepancy in a relatively high-order moment to small deviations of the balance from its design mass distribution.

(3) Ring attracting mass with the augmented balance. The vanishing of the first three derivatives of the change in gravitational field at the position of the torsion balance when the source mass ring is transported occurs only if the ring is manufactured exactly to design dimensions, is made of perfectly homogeneous materials, and is located exactly in its design position and orientation. To determine the effect on our experiment of deviations from these ideal ring conditions we made two studies. One study, discussed in detail in Sec. IV F, used Monte Carlo calculations to propagate the the effects of various assumed ring imperfections, determining their joint effect on the measured signal. The second study, discussed here, was based on measurements of the torque signal produced by the ring mass when transported about the augmented balance with its artificially large known mass multipole moments, yielding information on the a_{lm} moments of the ring. The dominant troublesome multipole coupling is expected to be to q_{21}. The augmented balance has by design a large q_{21} but no deliberate q_{31}. Hence, in measuring the response of the balance to the ring's transport we determine the critical Δa_{21} of the ring, but not the less critical Δa_{31}.

For this study the ring was transported about the augmented balance at 30° intervals, in five runs. Between runs the ring was rehung at various orientations about its symmetry axis as was done during the actual experiment. The rms value of Δa_{21} determined from the five runs was 4.3×10^{-10} s^{-2}. Using this in Eq. (9) together with the measured value of q_{21} for the unmodified balance leads to a possible contribution of 0.7 nrad to the $\Delta\theta$ signal from this dominant component of Newtonian ring-balance couplings, or 0.5 nrad for the possible rms contribution to a signal of the phase which would be associated with an anomalous force.

(4) Cube attracting mass with augmented balance. Runs of this type, in which the signal was large and predictable, served to test our analysis techniques and to calibrate the balance angular displacement readout system. The lead cube was moved in 30° steps for six revolutions around the balance, in three runs with the cube at three different heights as described in Sec. IV E 2. From the calculated values of the a_{lm} for the lead cube at its various heights together with the mean measured values of the balance θ for the various cube positions, the measured values of the q_{lm} of the augmented balance were determined. In doing so, the calibration factor for the balance angular readout system was adjusted so that the resulting value for the magnitude of q_{21} agreed with the expected value. This adjustment required that the assumed calibration factor be changed by 16% from the value determined by steering the optical lever mechanically by a calculated angle prior to the runs.

The resulting measured complex values $|q|e^{i\phi}$ of the q_{lm} of the augmented balance are presented in Table III, where they are compared with their expected values. The expected values are the sum of two contributions: the large values calculated for the moment contributions of the added copper posts of the augmented balance, and the much smaller q_{lm} values of the unmodified balance determined experimentally earlier.

The copper posts added to produce the augmented balance give it large moments for q_{21}, q_{32}, and q_{33} but should not contribute to q_{22} and q_{31}. As stated above, the overall scale factor of the measured q_{lm} has been ad-

TABLE II. Mass multipole moments of the unmodified (nominally symmetric balance), determined from runs using a lead cube as attracting mass.

l	m	$\lvert q\rvert$	l	m	$\lvert q\rvert$
2	1	0.029±0.002 g cm^2	3	1	0.27±0.07 g cm^3
2	2	0.025±0.001 g cm^2	3	2	0.039±0.037 g cm^3
			3	3	0.013±0.009 g cm^3

TABLE III. Comparison of measured and expected multipole moments of the augmented balance formed by adding copper posts to the nominally symmetric balance. The expected moments are those of the added copper posts plus the small measured moments of the unmodified balance. The overall calibration factor for the measured q_{lm} has been adjusted to reproduce the expected magnitude of q_{21}. Units are g cm^l.

l	m		Measured q_{lm} of unmodified balance	Calculated q_{lm} for posts[a]	Net expected q_{lm} for augmented balance[a]	Measured q_{lm} for augmented balance
2	1	$\|q\|$	0.029±0.002	3.42	3.44	≡3.44±0.01
		ϕ	162°±4.6°	150°	150.1°	150.2±0.1°
2	2	$\|q\|$	0.025±0.001	0	0.025	0.019±0.0004
		ϕ	0°±1.1°		0°	26°±4°
3	1	$\|q\|$	0.27±0.07	0	0.27	0.54±0.43
		ϕ	124°±10°		124°	52°±51°
3	2	$\|q\|$	0.04±0.04	5.74	5.72	5.58±0.06
		ϕ	4°±103°	120°	119.6°	120.3±0.3°
3	3	$\|q\|$	0.01±0.01	3.96	3.95	3.93±0.02
		ϕ	72°±40°	−90°	−89.9	−84.9±0.1°

[a]Uncertainties for the q_{lm} moments of the added posts were not estimated.

justed to give agreement with the expected value for q_{21}. Comparison of the measured phase of q_{21}, and phase and magnitudes of q_{32} and q_{33}, with their expected values then provides a test of our analysis procedures and of the sensitivity of the instrumentation. It will be noted in Table III that the magnitudes of q_{32} and q_{33} agree with expectation to within 3% and 1%, respectively; the phases of q_{21} and q_{32} are within 0.7° of expectation, while the phase of q_{33} is off by 5°. The large uncertainty in the measured (nominally zero) value of q_{31} reflects inaccuracies in knowledge of the vertical position of the lead cube in the various runs, which result in a part of the large signal contribution from q_{21} being misinterpreted in the fit as a contribution from q_{31}.

Figure 9 shows the measured response of the balance to the lead cube for three cube heights (with the overall scale factor discussed), comparing these measured values with those predicted by Eq. (7) using q_{lm} values calculated from the mass distribution of the augmented balance plus the small measured values of the unmodified symmetric balance. The measured response points are the result of signal averaging data from six full revolutions of the lead cube about the balance, after subtracting a linear drift from the data.

F. Newtonian gravitational couplings: Monte Carlo estimates

To supplement the tests described in the previous section, estimates of the coupling to the balance of Δa_{lm} moments associated with irregularities in the mass ring were made based on Monte Carlo studies of the magnitudes of these moments implied by ring irregularities consistent with measured limits on the ring's inhomogeneity and geometrical asymmetry. First, 1000 simulated experiments were analyzed in which a point mass equal to one-thousandth of the total ring mass was randomly placed in the volume of the lead ring. This level of homogeneity perturbation was at least as great as the maximum effective inhomogeneity that would be consistent with the ultrasound scans made of the lead components of the ring. For each experiment a set of Δa_{lm} values was calculated, and their rms value for the thousand experiments determined for each l and m. Second, 400 simulated experiments were analyzed in each of which the rings's position and orientation were perturbed by selecting parameters from Gaussian distributions with widths corresponding to the uncertainties indicated in Table IV. (Contributions to the Δa_{lm} from geometrical imperfec-

TABLE IV. Errors in ring positioning and orientation.

Radius of circle in which ring is transported	±0.01 cm
Balance horizontal position relative to the ring	±0.04 cm
Balance vertical position relative to the ring	(0.06±0.03) cm
Ring inclination toward balance	$\pm 2\times 10^{-4}$ rad
Ring rotation around its vertical symmetry axis	$\pm 2\times 10^{-3}$ rad
Tilt angle of ring transport turntable	$\pm 6\times 10^{-4}$ rad
Rotation positioning error of turntable ($\Delta\Psi$)	$\pm 4\times 10^{-4}$ rad

TABLE V. Estimated apparent signal contributions due to ring positioning errors and plausible mass inhomogeneity, based on Monte Carlo calculations.

l	m	Estimated Δa_{lm} (positioning) $s^2\ cm^{(2-l)}$	Estimated Δa_{lm} (defects) $s^{-2}cm^{(2-l)}$	Estimated net Δa_{lm} $s^{-2}\ cm^{(2-l)}$	Equivalent anomalous signal $\Delta\theta$ (nrad)
2	1	1.9×10^{-10}	3.6×10^{-10}	4.1×10^{-10}	0.24
2	2	1.7×10^{-10}	0	1.7×10^{-10}	0.17
3	1	1.1×10^{-11}	1.3×10^{-11}	1.7×10^{-11}	0.12
3	2	1.1×10^{-11}	0	1.1×10^{-11}	0.02
3	3	3.6×10^{-11}	1.1×10^{-11}	3.8×10^{-11}	0.03
		Net gravitational coupling uncertainty:			0.32 nrad

tion in ring manufacture were small compared to those from errors in ring position and orientation.) Root-mean-square values of the Δa_{lm} determined by this set of experiments were added in quadrature to those determined by the mass inhomogeneity experiments to give a net effective Δa_{lm} set. These separate and combined moments are tabulated in Table V along with the corresponding contributions to an equivalent anomalous force signal of the proper phase. Finally, adding in quadrature the signal contributions from the various moments, we obtained an estimate of 0.3 nrad for the uncertainty in anomalous force signal to be assigned to Newtonian couplings. For our error budget we take the gravitational coupling uncertainty to be the larger value of 0.5 nrad inferred in Sec. IV E, based on measured couplings of the ring to the q_{21} of the augmented balance.

G. Calibration uncertainty

The response of the autocollimator to balance rotation was calibrated before each data run using motor-driven micrometers to shift by known amounts the lateral position of a plate which held the LED source and split photodiode detector in the focal plane of the autocollimator. This "micrometer method" simulates a rotation of the balance mirror by a known amount. The calibration factor determined in this way was constant to within 5% over the period during which anomalous force data was taken in this experiment, but varied by as much as ±20% over the full period of the experimental work including the various tests for systematic effects. A check of this calibration method based on comparison of predicted and expected signals when a lead cube was transported around an augmented balance (see Sec. IV E) gave a calibration factor differing by 16%. Our final results are based on the calibrations using the "micrometer method," to which we assign an uncertainty of 20%. If these calibrations are in error in the direction suggested by the multipole coupling checks, then we have underestimated the sensitivity of our experiment and overestimated the values of the potentially troublesome multipole moments of the balance.

V. FINAL ANALYSIS

The final error budget for our experiment is presented in Table VI. After compiling an error budget[22] we revealed and subtracted the "hidden number" X used in our blind data analysis discussed in Sec. III B. Our final measure of an anomalous signal of the form $\Delta\theta(\Psi)=A_5\sin\Psi$ is given by $A_5=3.2\pm3.5$ nrad. The amplitude A_5 corresponds to the change in the equilibrium angle of the balance when the ring is moved from one side of the balance to the other along the axis of maximum sensitivity to an anomalous force. Figure 10 displays the corresponding function $A_5\sin\Psi$ along with the experimental data for data sets I and II separately [Fig. 10(a)] and averaged over the two data sets [Fig. 10(b)].

To interpret our results in terms of a single Yukawa potential of the form of Eqs. (1) and (2), it is convenient to write the torque on the balance as

$$\tau^5=-\xi\mathbf{p}^5\times\mathbf{g}^5\ , \tag{13}$$

where

$$\mathbf{p}^5\equiv\sum_i q_i\mathbf{p}_i\ , \tag{14}$$

where $\mathbf{p}_i$ is the dipole moment of the ith component of the test masses in the torsion balance and q_i is its corresponding anomalous charge defined by Eq. (2), and

$$\mathbf{g}^5\equiv\sum_i q_i\mathbf{g}_i^N\ , \tag{15}$$

where $\mathbf{g}_i^N$ is the contribution to the "Newtonian" gravita-

TABLE VI. Error budget summary.

Effect	Signal uncertainty (nrad)
Magnetic	0.03
Tilt	0.2
Gravitational	0.5
Thermal	2.2
Suspension asymmetry	0.25
Electronic coupling	1.5
Calibration uncertainty	0.6
Total systematic	2.8
Statistical	2.1
Total:	3.5

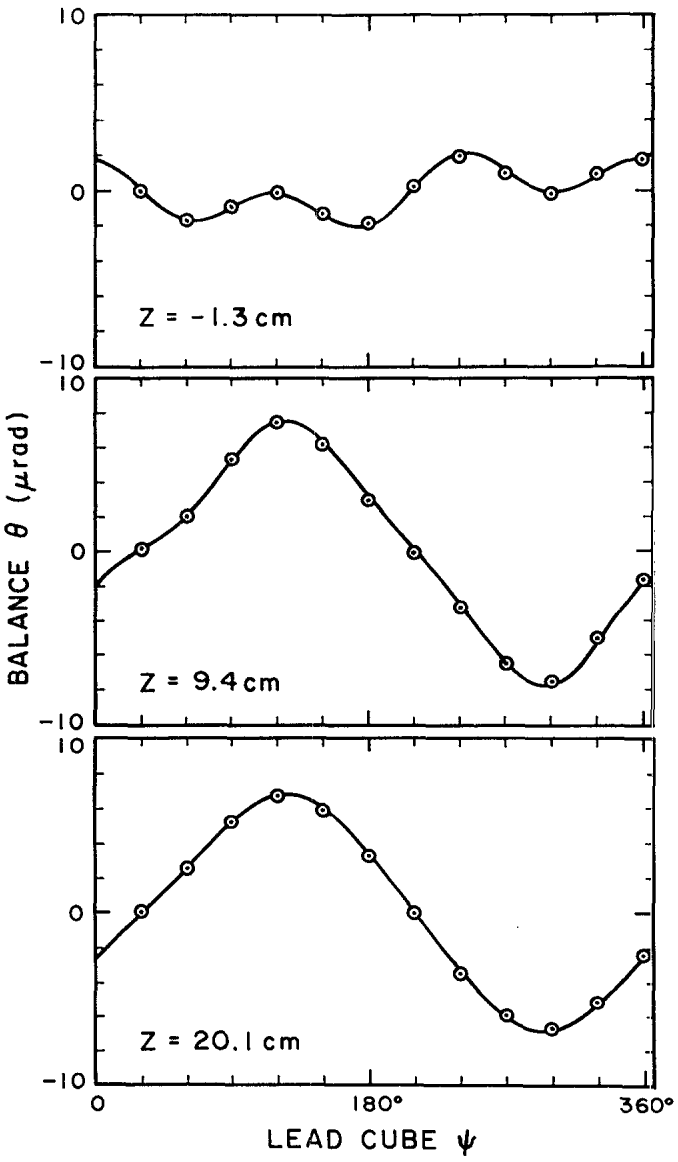

FIG. 9. A test of analysis procedures and apparatus sensitivity: response of the balance with added copper posts to a 40-kg lead cube at three different heights. Data points are the average of data from six cube revolutions, after subtraction of linear drift. The common calibration factor for the three plots has been adjusted to give a measured q_{21} moment in agreement with expected value. The solid lines are the expected balance θ response computed using Eq. (7) and the expected multipole moments of the augmented balance through $l=3$.

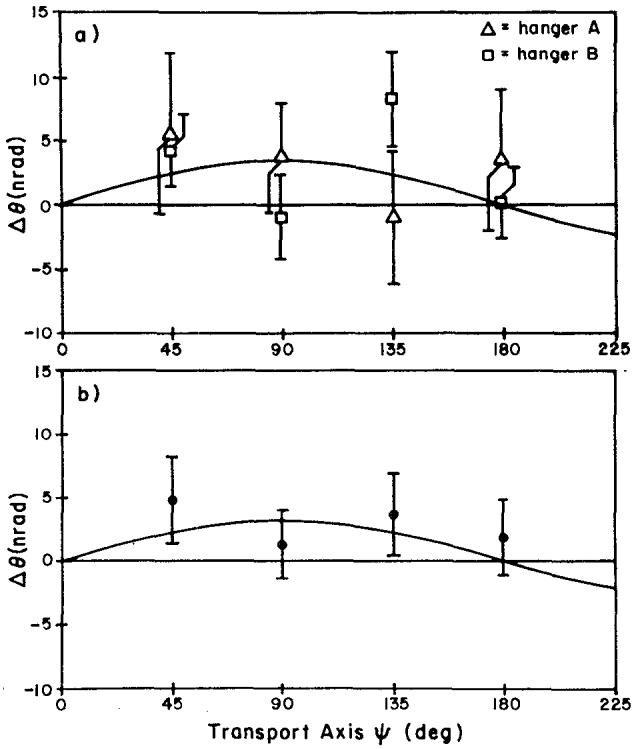

FIG. 10. Balance response $\Delta\theta$ to ring transport as a function of initial ring position ψ. (a) Response averaged separately for data taken with ring supported from hangers A and B, 180° apart on the transport turntable. (b) Unweighted average of the data from the two ring positions relative to the turntable. The solid curve is the fit of $A_5\sin\psi$ to the data of (b).

tional field at the position of the balance due to the ith component of the attracting mass ring, and q_i is the anomalous charge of that source component. In computing the "Newtonian" field $\mathbf{g}_i^N$, the Yukawa factor $e^{-r/\lambda}$ is to be included in the gravitational potential [or equivalently, the factor $(1+r/\lambda)e^{-r/\lambda}$ is to be included in the force field calculation]. The minus sign in Eq. (13) reflects the fact that the anomalous force is repulsive if the product $\xi q_1 q_2$ is positive.

Tables VII and VIII present the ingredients of $\mathbf{p}^5$ and $\mathbf{g}^5$ for our experiment, in a coordinate system such that the x axis points from the balance toward the ring, with the ring at $\Psi=0$.

From the ingredients in Tables VII and VIII we find

$$\mathbf{p}^5=(0.00\,622\cos\theta_5-0.689\sin\theta_5)\hat{\mathbf{x}}\ \text{g cm}\ , \tag{16}$$

$$\mathbf{g}^5=(1.53\cos\theta_5+0.282\sin\theta_5)\times10^{-5}\hat{\mathbf{x}}\ \text{cm s}^{-2} \tag{17}$$

TABLE VII. Components of the test mass dipole moments.

Test mass component	B/μ	$(N-Z)/\mu$	Dipole moment
Copper	1.00 895	0.08 908	$6.488\hat{\mathbf{x}}$ g cm^2
Lead	1.00 794	0.21 031	$-5.921\hat{\mathbf{x}}$ g cm^2
Aluminum	1.00 852	0.03 735	$-0.567\hat{\mathbf{x}}$ g cm^2

TABLE VIII. Contributions of ring components to the Newtonian field at the position of the balance. Ring is assumed to be at $\Psi=0$.

Ring component	B/μ	$(N-Z)/\mu$	$\mathbf{g}^N$ at balance
Lead	1.00794	0.21031	$1.300\times10^{-5}\hat{\mathbf{x}}$ cm s^{-2}
Aluminum	1.00852	0.03735	$0.204\times10^{-5}\hat{\mathbf{x}}$ cm s^{-2}
Brass	1.00895	0.08743	$0.010\times10^{-5}\hat{\mathbf{x}}$ cm s^{-2}
TOTAL			$1.514\times10^{-5}\hat{\mathbf{x}}$ cm s^{-2}

for the ring at $\Psi=0$ (on the plus x axis), and

$$\mathbf{g}^5=(1.53\cos\theta_5+0.282\sin\theta_5)\times10^{-5}(\cos\psi\hat{\mathbf{x}}+\sin\psi\hat{\mathbf{y}})\ \text{cm s}^{-2} \quad (18)$$

for the ring at an arbitrary Ψ. Equation (13) then becomes

$$\tau(\psi)=-\xi(0.00622\cos\theta_5-0.689\sin\theta_5)\times(1.53\cos\theta_5+0.282\sin\theta_5)\times10^{-5}\sin\psi\hat{\mathbf{z}}\ \text{dyn cm}\ . \quad (19)$$

Now the measure A_5 of anomalous signal determined from our data is related to the anomalous torque on the balance as a function of Ψ by

$$\tau(\psi)=\tfrac{1}{2}kA_5\sin(\psi)\hat{\mathbf{z}}\ , \quad (20)$$

where k is the torsion constant of the balance torsion fiber. [The factor of $\frac{1}{2}$ arises because A_5 defined via Eqs. (10) and (11) is a peak-to-peak θ signal amplitude.] Comparing Eqs. (19) and (20), using $A_5=3.2\pm3.5$ nrad and $k=0.070$ dyn cm/rad then leads to the values for ξ presented in the following section.

VI. CONCLUSION

A model-independent statement of our final result is the following: the fractional difference in apparent gravitational force per unit mass on two test masses, one of

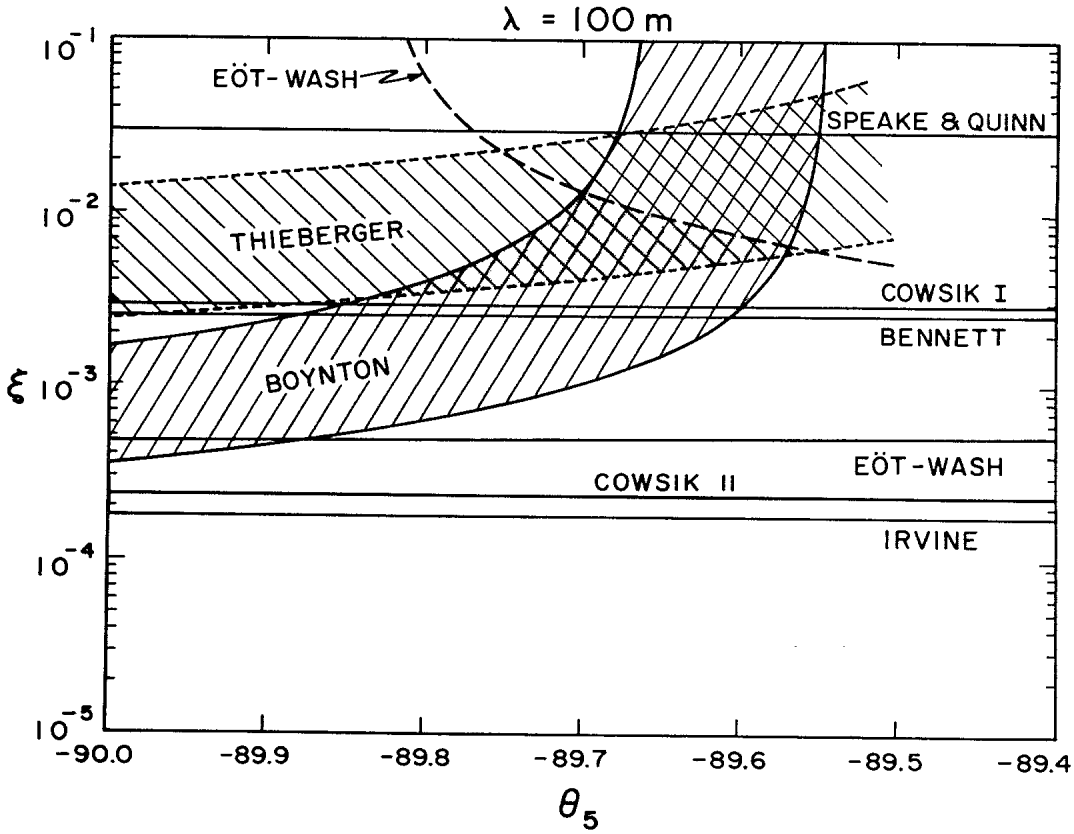

FIG. 11. Constraints at a 2σ level on an anomalous force coupling approximately to isospin. The positive effect bands labeled Thieberger (Ref. 4) and Boyton *et al.* (Ref. 5), and the curved Eöt-Wash (Ref. 6) upper limit, are based on experiments using geological source masses and depend on the assumed force range λ (taken here to be 100 m). The curves for these three experiments were calculated by Talmadge (Ref. 23). The horizontal 2σ upper limit labeled Bennett (Ref. 14) is approximately independent of λ for $\lambda>100$ m while the experiments labeled Speake and Quinn (Ref. 12), Cowsik I (Ref. 13), Cowsik *et al.* II (Ref. 18) Eöt-Wash (Ref. 8), and Irvine (this work) are based on experiments using a controlled local source mass, and are nearly independent of assumed range for $\lambda>1$ m.

copper and the other 91.5% lead and 8.5% aluminum by weight, due to an attracting mass at an average distance of 35 cm made of 87% lead, 12% aluminum, and 1% brass, is $(1.1\pm1.2)\times10^{-6}$, with the positive central value corresponding to a greater attractive force on the copper test mass. Equivalently, the acceleration of the copper test mass to the attracting source would be greater than that of the lead and/or aluminum test mass by $(1.7\pm1.9)\times10^{-11}$ cm/s^2.

Is we assume a Yukawa potential for a composition-dependent force of the form of Eq. (1), our results imply

$\xi=(5.7\pm6.3)\times10^{-5}$ for $\theta_5=90°$ ($N-Z$ coupling),

$\xi=(-1.2\pm1.3)\times10^{-3}$ for $\theta_5=0°$ (B coupling).

Figure 11 displays two standard deviation limits on $\xi(\theta_5)$ for values of θ_5 near $-90°$ obtained from our experiment and other recent experiments, for an assumed force range of 100 m. The shaded region in Fig. 11 is a region in parameter space in which it was pointed out by Boyn-

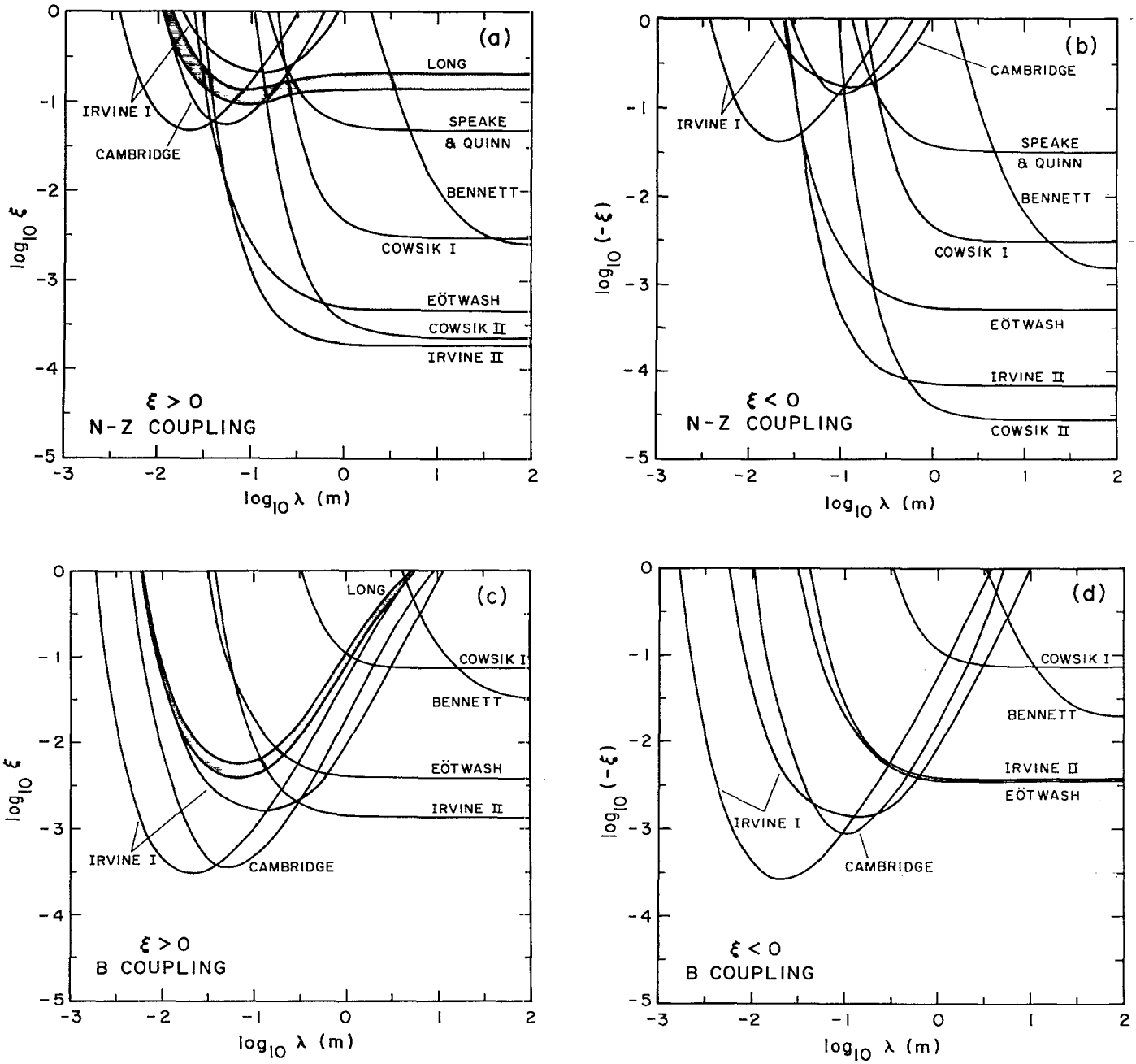

FIG. 12. Limits at a 2σ level on an anomalous force coupling strength ξ as a function of range λ for a single Yukawa potential of the form of Eq. (1), for $N-Z$ coupling [(a) and (b)] and B coupling [(c) and (d)]. The shaded band represents the *one*-standard-deviation limits corresponding to a nonzero effect reported by Long (Ref. 25) in a test of the gravitational inverse-square law. The 2σ limit curves labeled Irvine I (Ref. 26), Cambridge (Ref. 27), and Long (Ref. 25) also derive from experiments designed as inverse-square law tests. The curve Irvine II represents this work; the other references are as in Fig. 11.

ton *et al.*[5] that (at the time of his publication) existing experimental results indicating a positive anomalous effect[4,5] and results showing no effect[6] could be marginally consistent. Since Boyton's publication, a number of results have been reported,[8,13,14] including this work, excluding this possibility. The region in (ξ,θ_5) parameter space defined by the results of Refs. 4–6 depends on λ, moving downward in Fig. 11 as the assumed value of λ is increased so that for λ less or greater than 100 m the inconsistency of recent results with those discussed by Boynton becomes, respectively, more or less extreme than that indicated in Fig. 11.

Figure 12 displays results of this and other experiments which have used controlled local source masses[24] to search for anomalous forces superimposed on gravity. Figures 12(a)–12(d) present limits on the strength ξ of an anomalous force as a function of assumed force range λ, for the cases of pure B coupling ($\theta_5=0°$) and pure $N-Z$ coupling ($\theta_5=90°$), and for positive and negative values of ξ. The experiment of Long,[25] which gave an indication of a deviation from the inverse-square distance dependence of the gravitational force, used different materials for the attracting mass at two different mass separations and hence may be interpreted as an indication of composition dependence of an anomalous force of long-range λ; Fig. 12 shows the 1-standard-deviation limits corresponding to Long's result. For both B coupling and $N-Z$ coupling, Long's results are inconsistent with results of several other experiments presented in Figs. 12(a) and 12(c). Results of other early experiments[26,27] which were designed as inverse-square law tests are reinterpreted in Fig. 12 in terms of the limits they place on a coupling specifically to B or $N-Z$, using information on the composition of attracting and test masses in those experiments.

ACKNOWLEDGMENTS

We gratefully acknowledge the contributions of the machinists who made this experiment possible: Zsigmond Sebestyen for the lead ring, Zach Halopoff for the torsion balance, and Ralph Kolbush and Herbert Juds. We thank the Zeiss Corporation for their contribution of precision metrology of our mass transport turntable. We are grateful to the undergraduates who helped with the experiment in various stages: David Sar, Alvin Wong, Brian Meadows, Selena Forman, Ray Whorton, and Matthew Harmon. The experiment was supported by the National Science Foundation, Grant No. PHY-8709770.

*Present address: JILA, Boulder, CO 80309-0440.

[1]R. V. Eötvös, D. Pekár, and E. Fekete, Ann. Phys. (Leipzig) **68**, 11 (1922).

[2]E. Fischbach, D. Sudarsky, A. Szafer, C. Talmadge, and S. H. Aronson, Ann. Phys. (N.Y.) **182**, 1 (1988).

[3]E. Fischbach, D. Sudarsky, A. Szafer, C. Talmadge, and S. H. Aronson, Phys. Rev. Lett. **56**, 3 (1986).

[4]P. Thieberger, Phys. Rev. Lett. **58**, 1066 (1987).

[5]P. E. Boynton, D. Crosby, P. Ekstrom, and A. Szumilo, Phys. Rev. Lett. **59**, 1385 (1987).

[6]C. W. Stubbs *et al.*, Phys. Rev. Lett. **58**, 1070 (1987).

[7]E. G. Adelberger *et al.*, Phys. Rev. Lett. **59**, 849 (1987).

[8]C. W. Stubbs *et al.*, Phys. Rev. Lett. **62**, 609 (1989).

[9]B. R. Heckel *et al.*, Phys. Rev. Lett. **63**, 2705 (1989).

[10]P. G. Bizzeti *et al.*, Phys. Rev. Lett. **62**, 2901 (1989).

[11]V. L. Fitch, M. V. Isaila, and M. A. Palmer, Phys. Rev. Lett. **60**, 1801 (1988).

[12]C. C. Speake and T. J. Quinn, Phys. Rev. Lett. **61**, 1340 (1988).

[13]R. Cowsik *et al.*, Phys. Rev. Lett. **61**, 2179 (1988).

[14]W. R. Bennett, Jr., Phys. Rev. Lett. **62**, 365 (1989).

[15]T. M. Niebauer, M. P. McHugh, and J. E. Faller, Phys. Rev. Lett. **59**, 609 (1987).

[16]K. Kuroda and M. Mio, Phys. Rev. Lett. **62**, 1941 (1989).

[17]P. E. Boynton *et al.*, in *Proceedings of the Xth Moriond Workshop* (Editions Frontieres, Gif-sur-Yvette, to be published).

[18]R. Cowsik, N. Krishnan, S. N. Tandon, and S. Unnikrishnan, Phys. Rev. Lett. **64**, 336 (1990).

[19]Extensive discussions of experiments in this field may be found in the proceedings of the annual Moriond Workshops for 1987 through 1990: *New and Exotic Phenomena,* proceedings of the XXIInd Rencontre de Moriond, Les Arcs, France, 1987, edited by O. Fackler and J. Tran Thanh Van (Editions Frontieres, Gif-sur-Yvette, 1987); *5th Force and Neutrino Physics,* proceedings of the XXIIIrd Rencontre de Moriond, Les Arcs, France, 1988, edited by O. Fackler and J. Tran Thanh Van (Editions Frontieres, Gif-sur-Yvette, 1988); *Tests of Fundamental Laws of Physics,* proceedings of the XXIVth Rencontre de Moriond, Les Arcs, France, edited by O. Fackler and J. Tran Thanh Van (Editions Frontieres, Gif-Sur-Yvette, 1989), and *Proceedings of the Xth Moriond Workshop* (Ref. 17).

[20]T. Goldman, R. J. Hughes, and M. M. Nieto, Mod Phys. Lett. A **3**, 1243 (1988).

[21]See, for example, J. D. Jackson, *Classical Electrodynamics,* (Wiley, New York, 1975). The application of this formalism to gravitational torques on a torsion balance was first presented by Christopher Stubbs and Eric Adelberger and their collaborators (Ref. 6).

[22]The error budget at the time that the blindfold was taken off our data analysis differed from the final budget in the following contributions: electronic coupling 8.7 nrad, gravitational coupling 0.9 nrad, and no contribution from calibration uncertainty was included.

[23]C. Talmadge (private communication).

[24]Experiments using topographical features as attracting mass source, including those of Refs. 5, 9, 11, and 17, put limits on a coupling to B which, for $\lambda > 10$ m, are more stringent than those shown in Fig. 12 derived from experiments using controlled local attracting masses.

[25]D. R. Long, Nature (London) **260**, 417 (1976).

[26]J. K. Hoskins, R. D. Newman, R. Spero, and J. Schultz, Phys. Rev. D **32**, 3084 (1985).

[27]Y. T. Chen, Alan H. Cook, and A. J. F. Metherell, Proc. R. Soc. London **A394**, 47 (1984).